The Reorganization Energy of Cytochrome *c* Revisited

Ingo Muegge,[†,§] Phoebe X. Qi,[‡,§,||] A. Joshua Wand,[*,‡] Zhen T. Chu,[†] and Arieh Warshel[*,†]

Department of Chemistry, University of Southern California, Los Angeles, California 90089-1062, and Department of Chemistry, Center for Structural Biology, State University of New York at Buffalo, Buffalo, New York 14260-3000

Received: August 14, 1996; In Final Form: November 6, 1996[⊗]

The solution structures of the reduced and oxidized forms of the cytochrome *c* are used to reevaluate the reorganization energy for oxidation of cytochrome *c*. This is achieved by using the linear response approximation in concert with the NMR structures as pseudo energy constraints. Alternative estimates, obtained using a free energy perturbation approach employing umbrella sampling and a continuum dielectric approach, are also provided. The reorganization energy obtained is larger than that previously estimated using crystal structures of the protein. Nevertheless, the present estimate remains significantly smaller than the corresponding reorganization energy in water (9−15 kcal mol^{-1} as compared to ≈37 kcal mol^{-1} in water) and the protein contribution to the reorganization energy is only 8−10 kcal mol^{-1}. This provides further support for the proposal that proteins assist in electron transfer reactions by reducing the relevant reorganization energies. The solution structures are also used to estimate the redox potential of cytochrome *c*. Several strategies are employed including a newly formulated scaled linear response approximation. The calculations agree reasonably well with the observed redox potential. Analysis of the group contributions to the reorganization energy and redox potential reveals a clear energetic linkage between these fundamental parameters of electron transfer and a redox-dependent surface feature likely to influence recognition of cytochrome *c* by its redox partners. Specifically, the rearrangement of Ile81 and other residues at the heme edge upon a change in oxidation state gives rise to a large contribution to both the redox potential and the reorganization energy. Finally this work is used to explore and illustrate the meaning of macroscopic dielectric models. It is shown that the "proper" dielectric constant depends strongly on the model used since it basically represents the implicit contributions of the given model rather than a fundamental physics. Thus we obtain different effective dielectric constants for different treatments of redox potential and reorganization energy.

1. Introduction

Electron transfer (ET) plays a central role in biological processes. One of the best-characterized proteins involved in biological ET is cytochrome *c*, and much has been learned about the overall properties that determine its redox potential and the rate constant for electron transfer between this protein and its redox partners. According to Marcus' theory, which treats the environment as a dielectric continuum, the activation free energy for an electron transfer reaction can be approximated by the expression

$$\Delta g^{\ddagger} = (\Delta G_0 + \lambda)^2/4\lambda \qquad (1)$$

where ΔG_0 is the free energy for the reaction and λ is the so-called reorganization energy that reflects the energy released when the product state is placed at the reactant equilibrium configuration and then allowed to relax to the product equilibrium configuration.[1−3] However, the detailed factors that determine the activation energy of such processes are still unclear and subject to extensive debate. In particular, it is not yet clear what is the actual value of the protein contribution to the reorganization energy.

The emergence of microscopic simulation approaches has made it possible to evaluate the role of protein structure in setting the reorganization energy and the driving force of interprotein electron transfer.[4−8] Electron exchange between reduced and oxidized cytochrome *c*[9,10] or between cytochrome *c* and a covalently attached metal[11] is among the systems most amenable to detailed study by computational and physical methods.[12,13]

In early studies, Churg et al.[4] converted the rather small difference between the crystal structures of the two redox states of tuna cytochrome *c*[14,15] to an estimate of the reorganization energy and found this energy to be quite small (6 kcal mol^{-1}). This finding is consistent with the idea that proteins reduce activation barriers by minimizing the corresponding reorganization energies.[4,16,17]

Kinetic measurements have provided useful information about the magnitude of the reorganization energies in biological electron transfer reactions (for review see Moser et al.[18] and Farid et al.[19]). Studies that involved systematic variation of ΔG_0 indicated that the λ's in bacterial reaction centers are rather small (15 kcal mol^{-1}). This is also consistent with free energy perturbation calculations.[6] On the other hand, kinetic studies of ET between cytochrome *c* and cytochrome *c* peroxidase[20] were interpreted in terms of larger λ's (37 kcal mol^{-1}). However, these latter experiments did not involve a systematic variation of ΔG_0 and could reflect the energetics of bringing the donor and acceptor to their optimal positions (see discussion in the Concluding Remarks section). Furthermore, studies of ET between cytochrome *c* and cytochrome b5 gave a much smaller reorganization energy (18 kcal mol^{-1}).[21]

* Authors to whom correspondence should be addressed.
† University of Southern California.
‡ State University of New York at Buffalo.
§ These authors contributed equally.
|| Present address: Department of Chemistry, University of Illinois, 600 South Methews Avenue, Urbana, IL 61801.
⊗ Abstract published in *Advance ACS Abstracts,* January 15, 1997.

S1089-5647(96)02478-9 CCC: $14.00

While the kinetic estimates of the reorganization energy of cytochrome *c* are far from being definitive, there is now structural evidence that the reorganization energy may be larger than that deduced from the crystal structures of tuna cytochrome *c*. Recent NMR-based investigations of the solution structure of the protein in its two redox states suggest much larger redox-dependent structure changes.[22−28] Thus it is now important to reevaluate the magnitude of the reorganization energy of cytochrome *c* and to attempt to relate specific contributions of the protein to this and other fundamental parameters such as the redox potential and molecular recognition of cytochrome *c* by its redox partners.

This work uses the solution NMR structures of cytochrome *c* to calculate the reorganization energy using two simulation methods: one is based on the linear response approximation (which will be referred to here as the LRA) and the other on a direct evaluation of the free energy functions. We will focus mainly on the LRA approach since this strategy provides a powerful way of introducing the structural constraints into the calculations. The structural information is also used for direct calculation of redox potentials and for a consistent assessment of the dielectric constants in different electrostatic models of the protein.

The Methods section outlines our LRA and free energy perturbation (FEP) approaches, which provide a clear microscopic way for evaluating the reorganization energy and for dissecting the protein contributions to this quantity. We also present a rough macroscopic estimate of the distance dependence of λ. In the Results and Discussion section we summarize our simulation results and discuss the contributions from different regions of the system. We also develop several macroscopic models for calculations of reorganization and redox energies and compare them with the corresponding microscopic results. This allows us to determine the "dielectric constants" that should be used in each macroscopic model in order to reproduce the corresponding microscopic results. Finally, the implications of our finding are discussed.

2. Methods

A. Free Energy Perturbation/Umbrella Sampling Formulation. The process of electron transfer from a donor, D, to an acceptor, A, can be considered as a surface crossing between the potential surface of the reactant state ($V_a = V(D_1A_2^+)$) and the potential surface of the product state ($V_b = V(D_1^+A_2)$). When the donor and acceptor are held at a distance R it is possible to write the rate constant for the ET reaction as

$$k = A(R)\exp[-\Delta g^{\ddagger}\beta] \tag{2}$$

where $\beta = 1/k_BT$ (here k_B is the Boltzmann constant and T is the temperature). The factor $\exp(-\Delta g^{\ddagger}\beta)$ expresses the probability (per unit time) that a long trajectory on V_a will result in a crossing of V_a and V_b. The activation energy $\Delta g^{\ddagger}$ can be approximated by eq 1 if one assumes that the solvent can be described by macroscopic electrostatic theory and if quantum mechanical nuclear effects are neglected, but even in this case it is not obvious how to deduce the relevant macroscopic reorganization energy. Thus, we would like to use a microscopic approach for a direct evaluation of both $\Delta g^{\ddagger}$ and the reorganization energy in eq 1. In order to do so, it is useful, following the approach introduced by Warshel and co-workers[29,30] to take the energy difference between V_b and V_a as a reaction coordinate (i.e., $X = V_b - V_a$) and evaluate the probability $\exp(-g_a(X)\beta)$ that the system has a given value of X during an infinitely long trajectory on V_a and also the corresponding probability $\exp(-g_b(X)\beta)$ for a trajectory on V_b. The activation energy $\Delta g^{\ddagger}$ is then obtained from the intersection of the g_a and g_b of Figure 1 (see ref 31 for more details).

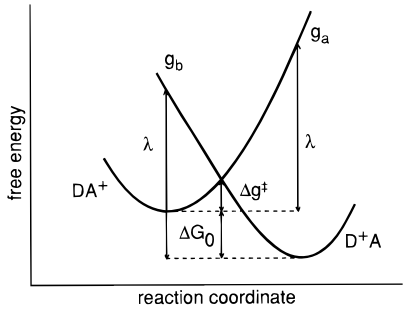

Figure 1. A schematic free energy surface for electron transfer reaction from a donor (D) to an acceptor (A^+). The activation energy $\Delta g^{\ddagger}$ is determined by the reorganization energy (λ) and the free energy difference ΔG_0. g_a, and g_b designate the free energy curves for the DA^+ and D^+A states, respectively.

As has been pointed out elsewhere,[6,29−32] it frequently is not practical to evaluate $\Delta g^{\ddagger}$ from very long trajectories on V_b and V_a. A much more effective approach is to use a combination of free energy perturbation (FEP) and umbrella sampling, where the configurational space is explored using a mapping potential of the form

$$V_m = V_a(1 - \theta_m) + V_b\theta_m \tag{3}$$

in which the mapping parameter θ_m is increased stepwise from zero to one. The free energy function for the system in state α (where α can be a or b) is given by[31]

$$g_\alpha(X_u) = -\beta^{-1}\ln[\langle\delta(X - X_u)\exp[-(V_\alpha(t) - V_m(t))\beta]\rangle_m P_m] \tag{4}$$

where X_u is a specific value of X, $\langle\ \rangle_m$ denotes a time average over a trajectory on m, the delta function $\delta(X - X_u)$ is assigned a value of 1 if $|X(t) - X_u| \le \Delta X/2$ and zero otherwise, and

$$P_m = \exp[-\Delta G_m\beta] = \prod_{n=0}^{m-1}\langle\exp[-(V_{n+1}(t) - V_n(t))\beta]\rangle_n \tag{5}$$

For a detailed explanation of this procedure we refer the reader elsewhere.[31]

Marcus' relationship (eq 1) is obtained if the free energy functions g_a and g_b are parabolic functions with equal curvature. Obviously there is no a priori reason to assume that eq 1 is rigorously valid in anharmonic systems. Unfortunately, it is difficult to examine the validity of this equation using direct experimental information. However, computer simulation studies based on equation 4 and related studies[6,29−33] have indicated that the assumption of quadratic free energy functions is a very reasonable approximation in the case of polar solvents and proteins and this approximation will indeed be exploited below.

B. Linear Response Approximation for Calculations of Reorganization Energies. The g_a and g_b that can be obtained from eq 4 should provide, at least in principle, the reorganization energy for electron transfer between cytochromes (see Figure 1). However, present simulation approaches involve significant sampling problems and cannot guarantee that the equilibrium geometries of the reactant and product state will be identical to the observed geometries. Since the present work is aimed at analyzing the relationship between the protein structures and the reorganization energies, it is important to introduce the structural information as a constraint in the calculation. The most straightforward way of doing this is provided by the LRA.

That is, assuming that the system can be described with the quasi harmonic approximation by many harmonic modes, one obtains[34,35]

$$\lambda = {}^1/_2[\langle V_b - V_a\rangle_a - \langle V_b - V_a\rangle_b] \quad (6)$$

$$\Delta G_0 = {}^1/2[\langle V_b - V_a\rangle_a + \langle V_b - V_a\rangle_b]$$

This means that the averages of the difference in potential energy between states b and a over trajectories on states a ($\langle V_b - V_a\rangle_a$) and b ($\langle V_b - V_a\rangle_b$)) can be used to obtain λ and ΔG_0. Note, that a and b correspond to two states (DA^+ and D^+A) of two cytochromes rather than just to the reduced and oxidized form of a single cytochrome. This complication will be addressed below.

An alternative derivation of the LRA results for ΔG_0 is obtained by using eq 4 for the case where θ is changed in a single step from 0 to 1. This gives[35,36]

$$\Delta G_0 = {}^1/_2\beta^{-1}[\ln\langle\exp[-\beta(V_b - V_a)]\rangle_a - \ln\langle\exp[-\beta(V_a - V_b)]\rangle_b] \quad (7)$$

Expanding eq 7 gives

$$\Delta G_0 = \frac{1}{2}\beta^{-1}\left[\beta\langle V_b - V_a\rangle_a + \beta\langle V_b - V_a\rangle_b + \frac{\beta^2}{2}\langle(V_b - V_a)^2\rangle_a + \frac{\beta^2}{2}\langle(V_b - V_a)^2\rangle_b + ...\right] \quad (8)$$

Retaining only the linear terms in $\langle V_b - V_a\rangle$ yields theΔG_0 of eq 6.

With the LRA approximation, one can introduce structural constraints in a simple way by replacing the average over V_α (i.e., $\langle\ \rangle_\alpha$) by an average over V_α and a constraint function that keeps the system near the observed coordinates of the αth state. That is, the calculations can be done using a potential of the form

$$V'_\alpha = V_\alpha + \sum_n K(r_{\alpha,n} - r^0_{\alpha,n})^2 \quad (9)$$

where n runs over all the atomic coordinates, $r^0_{\alpha,n}$ is the observed nth coordinate of the αth state of the system, $r_{\alpha,n}$ is the nth coordinate in a given structure, and K is the force constant. Then

$$\lambda = {}^1/_2[\langle V_b - V_a\rangle_{a'} - \langle V_b - V_a\rangle_{b'}] \quad (10)$$

This procedure forces the model structures corresponding to the potentials V'_a and V'_b to stay close to the experimentally observed structures where $\langle\ \rangle_{a'}$ designates an average over V'_a. Since states a and b correspond to two states (DA^+ and D^+A) of a complex composed of two cytochromes, **r** spans the dimensionality of the two proteins so that $\mathbf{r}^0_a = (\mathbf{r}^0_{red},\mathbf{r}^0_{ox})$ and $\mathbf{r}^0_b = (\mathbf{r}^0_{ox},\mathbf{r}^0_{red})$ where $\mathbf{r}^0_{red}$ and $\mathbf{r}^0_{ox}$ are the refined solution structures of reduced and oxidized cytochrome *c*.

Because we deal with an exchange reaction between two identical cytochromes, we can rewrite eq 10 for the situation where the two cytochromes are held at infinite distance from each other as

$$\lambda^\infty = \langle V_{ox} - V_{red}\rangle_{red'} - \langle V_{ox} - V_{red}\rangle_{ox'} = \langle\Delta V\rangle_{red'} - \langle\Delta V\rangle_{ox'} \quad (11)$$

where $\langle\ \rangle_{red'}$ designates an average over trajectories on the potential V'_{red} of the type used in eq 9, but now V involves only a single protein with $\mathbf{r}^0_{red}$ taken as the refined structure of the cytochrome, while $\langle\ \rangle_{ox'}$ is obtained in the same way with V'_{ox}.

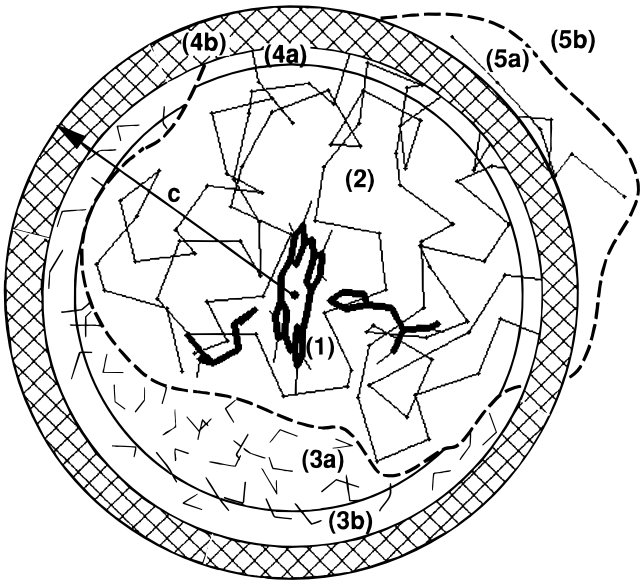

Figure 2. A schematic description of the five regions used in the surface constrained all atom solvent (SCAAS) modeling of the cytochrome *c*. Region 1 contains the heme and its ligands. Region 2 contains the protein groups (constrained with the force constant *K*) within a radius $\bar{b}$ from the center of the system. Region 3a contains the unconstrained water molecules and region 3b contains the surface water molecules (which are subjected to surface polarization constraints). Region 4a contains the harmonically constrained protein atoms between the radii $\bar{b}$ and $\bar{c}$. Region 4b contains the grid of Langevin dipoles that complete regions 1, 2, 3, and 4a to a sphere of radius $\bar{c}$. Region 5 is modeled as a dielectric continuum including region 5a of the protein and the solvent 5b beyond region 4 (see ref 38 for more details). For the sake of clarity we list here several energy terms that correspond to the different regions of the protein−water system. $\lambda^\infty_{1-5} \equiv \lambda^\infty$ represents the total reorganization energy of the system upon ET at infinite separation of donor and acceptor where 1−5 designates contributions from regions 1-5. λ^∞_{1-4} represents the contributions of regions 1−4 to the reorganization energy, and λ^∞_5 contains contributions of region 5 calculated by using the generalized Born approximation. $\lambda^R_{1-5} \equiv \lambda^R$ represents the corresponding energy at a distance R between donor and acceptor. λ_{1-2} is the contribution to λ^R that comes from the interaction of the heme with its ligands and the protein. λ_p is λ_{1-2} without the interaction between the heme and its ligands. λ^∞_{3-5} (λ^R_{3-5}) is the solvent contribution to λ^∞(λ^R) at infinite (finite) separation of donor and acceptor.

The potential surface used in our simulation studies employs a microscopic representation of the protein and its surrounding solvent shell up to a radius $\bar{c}$ and a continuum representation for the rest of the bulk solvent. This division into microscopic and macroscopic regions is described in Figure 2 that also considers the subdivision of the microscopic region (more details about these regions are given in the Results and Discussion section). The bulk contribution to the solvation of a single oxidized cytochrome, ΔG^{bulk}_{sol} can be evaluated using Born's formula

$$\Delta G^{bulk}_{sol} = -166\left(\frac{1}{\bar{c}}\right)\left(1 - \frac{1}{\epsilon_w}\right) \quad (12)$$

where the solvation energy is given in kcal mol^{-1} and $\bar{c}$ in angstroms. In our treatment we allow the bulk contribution to relax instantaneously with any heme charge distribution. The ΔV term (eq 11) that would have been obtained by the LRA with a real polar solvent in the bulk region can be easily estimated. However, as far as the reorganization energy is

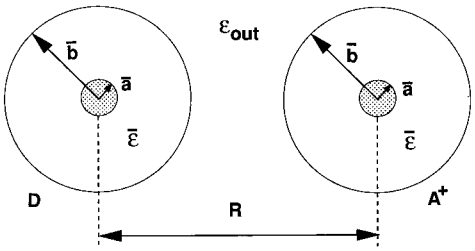

Figure 3. Schematic representation of a continuum model for electron transfer between two proteins. The cofactor is represented by a sphere of radius $\bar{a}$ surrounded by a hypothetical protein of radius $\bar{b}$ (and having a dielectric $\bar{\epsilon}$) immersed in a continuum of a dielectric ϵ_{out}.

concerned we can evaluate the bulk contribution using the continuum estimate[37]

$$\lambda_{bulk}^{R} = 332\left(\frac{1}{\epsilon_{op}} - \frac{1}{\epsilon_{w}}\right)\left(\frac{1}{\bar{c}} - \frac{1}{R}\right) \tag{13}$$

where R is the distance between the two cytochromes, ϵ_{op} is the dielectric constant of the molecules in the bulk region at very high frequencies (here we take $\epsilon_{op} \cong 2$), and $\epsilon_{w} \cong 80$. Using eqs 12 and 13 and the approximation $\epsilon_{op} \cong 2$, one obtains

$$\lambda_{bulk}^{R} = \lambda_{5}^{R} = \left(-\Delta G_{sol}^{bulk} - \frac{166}{\bar{c}\epsilon_{w}}\right)\left(1 - \frac{\bar{c}}{R}\right) \cong -\Delta G_{sol}^{bulk}\left(1 - \frac{\bar{c}}{R}\right) \tag{14}$$

where λ_{5}^{R} is the contribution of region 5 (the bulk region) of Figure 2. This equation can be extended in principle to represent the explicit water molecules around the protein (see below).

The total reorganization energy of the system can be written now as

$$\lambda_{1-5}^{\infty} = \lambda_{1-4}^{\infty} + \lambda_{5}^{\infty} = (\langle \Delta V^{1-4} \rangle_{red'} - \langle \Delta V^{1-4} \rangle_{ox'}) - \Delta G_{sol}^{bulk} \tag{15}$$

where 1−4 designates the contributions from regions 1 to 4 in Figure 2 without the contribution of the surrounding bulk (region 5). Equation 15 is only introduced as a practical trick of treating the bulk contribution of region 5. The other contributions of the internal regions of Figure 2 are evaluated microscopically and their determination is quite important for elucidating the protein contributions to λ (these contributions are discussed in subsequent sections).

C. Continuum Estimates of the Distance Dependence of Reorganization Energies. The analysis presented above is aimed at determining λ^{∞}. As to the distance dependence of λ, the situation is more complicated and far less unique. In the absence of the structure of the donor−acceptor complexes it is not fully justified to perform calculations on an assumed complex configuration. Indeed, the assumption that a specific donor−acceptor complex exists is unjustifiable. Thus we will estimate λ_{1-5}^{R} using a macroscopic approach. This estimate is based on the model considered in Figure 3 where the protein is represented by a sphere of a uniform dielectric and radius $\bar{b}$ around a heme that is represented by a sphere of a radius $\bar{a}$. To evaluate the reorganization energy for an electron transfer from D to A^+, we start by assuming that the dielectric constant of the solvent around the protein ϵ_{out} is equal to the protein dielectric $\bar{\epsilon}$ and we then obtain the reorganization energy by the standard formula for ET between two spheres in a uniform dielectric[37] (eq 13),

$$\lambda(\epsilon_{out} = \bar{\epsilon}) = 332\left(\frac{1}{2} - \frac{1}{\bar{\epsilon}}\right)\left(\frac{1}{\bar{a}} - \frac{1}{R}\right) \tag{16}$$

$$= 332\left(\frac{1}{2} - \frac{1}{\bar{\epsilon}}\right)\left[\left(\frac{1}{\bar{a}} - \frac{1}{\bar{b}}\right) + \left(\frac{1}{\bar{b}} - \frac{1}{R}\right)\right] \tag{17}$$

where we assume for simplicity that $\epsilon_{op} = 2$ and where we divide the contribution to λ to the inner and outer regions. In the next step, we calculate the change in reorganization energy of the outer region (beyond the radius $\bar{b}$) upon change of ϵ_{out} from its current value ($\epsilon_{out} = \bar{\epsilon}$) to its actual value (i.e., $\epsilon_{out} = 80$). This gives

$$\Delta\lambda[(\epsilon_{out}{=}\bar{\epsilon}) \rightarrow (\epsilon_{out}{=}80)] = 332\left[\left(\frac{1}{\bar{\epsilon}} - \frac{1}{80}\right)\left(\frac{1}{\bar{b}} - \frac{1}{R}\right)\right] \tag{18}$$

Thus, the actual λ is given by

$$\lambda = \lambda(\epsilon_{out}{=}\bar{\epsilon}) + \Delta\lambda = 332\left[\left(\frac{1}{2} - \frac{1}{\bar{\epsilon}}\right)\left(\frac{1}{\bar{a}} - \frac{1}{\bar{b}}\right) + \left(\frac{1}{2} - \frac{1}{80}\right)\left(\frac{1}{\bar{b}} - \frac{1}{R}\right)\right] \tag{19}$$

This estimate can be written as

$$\lambda_{1-5}^{R} = \left(\frac{166}{\bar{a}}\right)\left(1 - \frac{\bar{a}}{\bar{b}}\right)\left(1 - \frac{2}{\bar{\epsilon}}\right) + \left(\frac{166}{\bar{b}}\right)\left(1 - \frac{\bar{b}}{R}\right)\left(1 - \frac{2}{80}\right)$$
$$= \lambda_{1-2} + \lambda_{3-5}^{\infty}\left(1 - \frac{\bar{b}}{R}\right) = \lambda_{1-2} + \lambda_{3-5}^{R} \tag{20}$$

where we use the approximation $\epsilon_{op} = 2$ and the effective radii $\bar{a}$ and $\bar{b}$ are determined by equating the microscopically evaluated λ's with the corresponding macroscopic estimate (i.e., $\lambda_{1-2} = (166/\bar{a})(1 - (\bar{a}/\bar{b}))(1 - 2/\bar{\epsilon})$) and $\lambda_{3-5}^{\infty} = (166/\bar{b})(1 - (2/80))$). The parameter $\bar{a}$ is taken as the effective heme radius as determined from the solvation energy. The $\bar{\epsilon}$ term is the assumed protein dielectric constant that will be discussed below, while $\bar{b}$ is the effective protein radius which is deduced from the calculated solvation energy of the protein. Here we use the assumption $R = 2\bar{b}$ to estimate λ^{R} (we use λ^{R} and λ_{1-5}^{R} as synonyms) and discuss the dependence of λ^{R} on R (see below). Equation 20 divides λ_{1-5} into the protein contribution λ_{1-2} and the solvent contribution λ_{3-5}. These contributions will be used in the subsequent sections in analyzing the relationship between microscopic and macroscopic estimates of λ.

Before leaving this section we would like to point out that our concrete analysis focused on λ^{∞} and the discussion of λ^{R} is much more tentative.

3. Results and Discussion

A. Estimating Reorganization Energies by the Linear Response Approximation. The LRA approach of the previous section provides a very powerful way of correlating observed structural changes with reorganization energies. Here we applied this formulation to the NMR coordinates of reduced and oxidized cytochrome *c* which are referred to here as $\mathbf{r}_{ox}^{0}$ and $\mathbf{r}_{red}^{0}$. The LRA calculations involved the use of the molecular simulation program ENZYMIX[38] with its standard force field and with heme charges determined by the QCFF/PI method.[39] The potential differences $\langle \Delta V \rangle_{ox'} - \langle \Delta V \rangle_{red'}$ were evaluated by introducing the constraints of eq 9 with either $\mathbf{r}_{ox}^{0}$ or $\mathbf{r}_{red}^{0}$ and running the corresponding trajectory for 11 ps at 300 K with time steps of 1 fs and using the last 9 ps for the LRA analysis. The calculations involve the SCAAS polarization boundary conditions and the local reaction field method[40] which provides a very efficient way of handling the long-range electrostatic interactions. The system used (Figure 2) includes the entire protein (regions 1 and 2) in a water sphere with a radius of 21 Å (region 3) surrounded by a shell with an outer

TABLE 1: Breakdown of Electrostatic Contributions to the Reorganization Energy Evaluated by the LRA Analysis of Ferri- and Ferrocytochrome *c*

	model 1 (K = 0.1, n, LPw[a])		model 2 (K = 50.0, n, LPw)		model 3 (K = 50.0, i, LPw)		model 4 (K = 0.1, n, Lw)	
	$\langle\Delta V\rangle_{red}$	$\langle\Delta V\rangle_{ox}$	$\langle\Delta V\rangle_{red}$	$\langle\Delta V\rangle_{ox}$	$\langle\Delta V\rangle_{red}$	$\langle\Delta V\rangle_{ox}$	$\langle\Delta V\rangle_{red}$	$\langle\Delta V\rangle_{ox}$
$\langle\Delta V_{QQ}\rangle$	−8.33	−12.08	−8.87	−12.46	−8.73	−12.23	−7.64	−12.04
$\langle\Delta V_{intra}\rangle$	22.28	22.22	22.62	22.53	−61.87	−69.09	22.27	22.29
$\langle\Delta V_{intra}^{prop}\rangle^b$					(−84.14)	(−91.38)		
$\langle\Delta V_{q\mu}^{p}\rangle$	2.82	−8.77	12.40	1.15	71.87	51.76		
$\langle\Delta V_{q\alpha}^{p}\rangle$	−16.25	−3.82	−18.95	−12.16	−15.15	5.91		
$\langle\Delta V_{q\mu}^{w}\rangle$	0.35	−8.37	−7.99	−9.05	4.11	−1.43	−5.44	−35.01
$\langle\Delta V_{q\alpha}^{w}\rangle$	0.41	1.13	0.23	0.54	−0.63	−0.48	−4.43	3.08
$\langle\Delta V_{LD}\rangle$	5.33	−0.08	5.04	−0.87	0.92	0.12	1.31	−3.95
ΔG_{sol}^{bulk}	−6.81	−6.96	−6.80	−6.90	6.81	6.77	−9.14	−9.18
λ_{1-5}^{∞}	23.26		21.65		9.17		40.86	

[a] LPw designates the ligand and the protein in water; Lw designates the ligand in water. The ligand consists of the heme and its Met80 and His18 ligands. n (neutral) means that the reduced heme and the ionizable residues of the protein are not charged. Standard enzymix atomic partial charges are assigned to the atoms of all residues. i (ionized) means that all residues of types Asp, Glu, and Lys (except residues 5, 22, 60, 87, 88, 99, and 100) and Arg38 are ionized. The unionized Lys residues are located at the surface of the protein and are relatively far away from the heme (the nearest is Lys60 which is more than 8.5 Å apart from any heme atom). All other residues are in their neutral state. The reduced heme is neutral in all models, but in the ionized model the two propionic acid side chains are negatively charged. In all models the overall system charge is zero. V_{QQ} is the Coulombic interaction between the heme, Met80, and His18 in vacuum. V_{intra} that does not include V_{QQ} is the Coulombic contribution that occurs within the heme, the Met80, and the His18 in vacuum. Note that, in the case of the twofold charged heme (ionized model), the interaction between the heme and the charged propionic acids (V_{intra}^{prop}) is included in V_{intra}. $V_{q\mu}^{p}$ is the Coulomb interaction between L and P in vacuum. $V_{q\mu}^{w}$ is the Coulomb interaction between L and the explicit water in vacuum. $V_{q\alpha}^{p}$ is the interaction between L and the induced protein dipoles. $V_{q\alpha}^{w}$ is the interaction between L and the induced water dipoles. V_{LD} is the interaction between the Langevin dipoles and L. ΔG_{sol}^{bulk} is the Born energy. All energies are given in kcal mol^{-1}. The protein atoms are harmonically constrained at their equilibrium position with the force constant K given in kcal mol^{-1} Å^{-2}. $\lambda_{1-5}^{\infty} = (\langle\Delta V_{QQ}\rangle + \langle\Delta V_{intra}\rangle + \langle\Delta V_{q\mu}^{p}\rangle + \langle\Delta V_{q\alpha}^{p}\rangle + \langle\Delta V_{q\mu}^{w}\rangle + \langle\Delta V_{q\alpha}^{w}\rangle + \langle\Delta V_{LD}\rangle)_{red} - (\langle\Delta V_{QQ}\rangle + \langle\Delta V_{intra}\rangle + \langle\Delta V_{q\mu}^{p}\rangle + \langle\Delta V_{q\alpha}^{p}\rangle + \langle\Delta V_{q\mu}^{w}\rangle + \langle\Delta V_{q\alpha}^{w}\rangle + \langle\Delta V_{LD}\rangle)_{ox} - {}^1/_2(\Delta G_{ox}^{bulk} + \Delta G_{red}^{bulk})$ (compare to eq 15). [b] The values in parenthesis represent the interaction between the charged propionic acids and the rest of the heme. They are estimated by subtracting the corresponding values of $\langle\Delta V_{intra}\rangle$ of the Lw calculations (model 4) from the calculated value of $\langle\Delta V_{intra}\rangle$.

radius of 25 Å containing a Langevin grid (region 4) and then a continuum representation beyond the 25 Å shell (region 5). The simulations were done for different models with constraint force constants (the K of eq 9) of both 50 kcal and 0.1 kcal mol^{-1} Å^{-2}. The energy contributions considered include interactions between the protein residual charges and the heme ($V_{q\mu}^{p}$), interactions between the heme and the explicit water ($V_{q\mu}^{w}$), interactions with induced dipoles ($V_{q\alpha}$), the contribution of the solvent molecules in the region modeled by Langevin dipoles (V_{qL}), and finally the free energy of the surrounding bulk water. The van der Waals contributions and the interaction of the protein itself with other parts of the protein and water are, of course, included in the molecular dynamics but do not contribute to $\langle V_b - V_a\rangle$. It is important to note that the Langevin dipoles do not include a term that represents atomic polarizability (although such a term is included in other studies[41]). Thus, the contribution from the Langevin region to the reorganization energy is somewhat overestimated. However, this effect is rather small (since the Langevin region is not large) and is neglected in the present study. Simulations were done for two protein models. The first model considers all the protein ionizable groups and the heme propionic acids in their neutral form. The second model considers all the ionizable groups in the ionization state (except those that are located far from the heme, see caption of Table 1 for details) that they will have if their pK_a is unchanged by the protein (relative to its value in water). In the latter case, the heme is 2-fold negatively charged while the total protein remains neutral. The calculations were also done for a reference system composed of the heme with its two ligands (His18 and Met80) in water, constraining the heme ligands system with $K = 0.1$ kcal mol^{-1} Å^{-2}. The results of the calculations with the different models are summarized in Table 1. It gives a breakdown of the individual contributions to the average of $(V_{ox} - V_{red})$ over trajectories generated by using the crystal structures of ferro- and ferricytochrome *c*, respectively. These contributions provide the raw data for the following analysis.

Using the LRA results and eqs 15 and 20 we obtained the reorganization energies of the systems. These reorganization energies are summarized in Table 2. Several points emerge from the table. The calculated reorganization energy λ_{1-5}^{R} ranges between 9.5 and 14.9 kcal mol^{-1} in the different protein models when the distance R between the two hemes is taken as 54 Å (this corresponds to approximately twice the effective radius of the protein). Most notable is the finding that λ^{R} in the protein is about one-third of the value for the heme−ligand system in water (37.2 kcal mol^{-1}). The distance dependence of λ_{1-5}^{R} as calculated using eq 20 for the neutral protein model is shown in Figure 4. As seen from the figure, λ depends on the distance in a significant way and this dependence should be considered in the interpretation of experimental information about biological ET. The dependence of λ^{R} on the distance in the case of the ionized protein model is quite small and is not shown in the figure. In this case, we consider the dependence obtained from eq 20 to be somewhat unreliable.[42] In general, we suggest considering the results of Figure 4 as only a rough estimate. The present approach is easily capable of evaluating λ for a donor and acceptor pair once their mutual orientation is known or assured. It is important to realize in this respect that the present solution structures of the reduced and oxidized cytochrome only provide direct information about the reorganization energy at infinite separation (λ^{∞}).

Another interesting point that emerges from our calculations is the intrinsic contribution of the protein residues to λ. This quantity was evaluated by taking into account only the contributions of $\langle V_{intra}^{p}\rangle$, $\langle V_{q\mu}^{p}\rangle$, $\langle\Delta V_{q\alpha}^{p}\rangle$, and $\langle\Delta V_{QQ}\rangle$ (see Table 2 for explanations of these terms). The six long-lived internal water molecules, detected by NMR, that are buried in the protein structures are treated as part of the protein (Table 2). The protein contribution to the reorganization energy λ_{1-2} is

TABLE 2: Calculated Reorganization Energies for Different Models Using the LRA Approach

model[a]	λ_{1-5}^{∞}	λ_{1-5}^{R}	λ_{1-2}	λ_p
model 1 ($K = 0.1$, n, LPw[b])	23.3	13.0	3.0	−0.8
model 2 ($K = 50.0$, n, LPw)	21.6	14.9	8.2	4.6
model 3 ($K = 50.0$, i, LPw[c])	9.2	9.5	9.8	6.3
model 4 ($K = 0.1$, n, Lw)	40.9	37.2[d] (22.6)	4.4	0.0

[a] Models are defined in Table 1. λ_{1-5}^{∞} was calculated using eq 15 (compare also Table 1). The distance between the centers of the donor and acceptor was taken as $R = 2\bar{b} = 54$ Å. The overall distance dependence of λ^R is discussed in the text and illustrated in Figure 4. λ_p designates the contribution to λ_{1-2} without V_{QQ}, which is the only non-zero non-water contribution for the Lw system (model 4) and stands for the interaction between the heme and its ligands His18 and Met80. (See Table 1.) λ_{1-2} includes the contributions from the six NMR-water molecules, which are treated in our calculations as part of the protein. Note that the contributions of these water molecules to the reorganization energy can be estimated from Figure 5. [b] The protein atoms are harmonically constrained to their positions with the force constant K (given in kcal mol^{-1} Å^{-2}). See Table 1. [c] The ionization state of the "ionized" system (model 3) is described in the caption of Table 1.[d] In order to compare the distance-dependent reorganization energies of the heme−ligand complexes in water and in the protein environment on equal footing, one has to consider λ_{1-5}^{R} at the same distance $R = 54$ Å in water and protein even though in water the ET is not likely to occur at this distance. However, it is noteworthy that even at a distance of $R = 2\bar{a} = 10.7$ Å between the hemes in water (value given in parenthesis) λ_{1-5}^{R} is still considerably larger in water than in the protein.

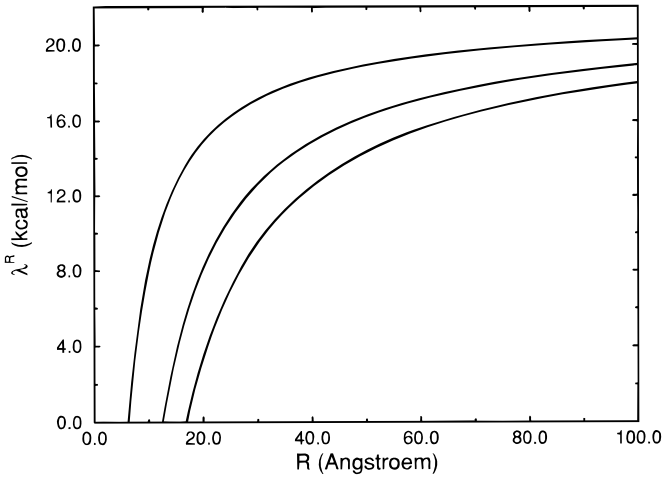

Figure 4. Distance dependence of λ^R. The results presented were obtained from eq 20 for the neutral protein model with $K = 50$ kcal mol^{-1} Å^{-2}. The calculations correspond to the values of $\bar{a} = 5.35$ Å and $\bar{b} = 10$, 20, and 27 Å from top to bottom. The curve for $\bar{b} = 27$ Å (bottom) corresponds to the value given in Table 2 ($R = 54$ Å). The assumption that the distance between the two cytochromes is $2\bar{b}$ represents an upper limit of R since it is likely that the cytochromes come close to each other in orientations where the heme-to-heme distance is smaller than $2\bar{b}$. In this context it is interesting to note that at $R = 30$ Å both the neutral and ionized protein models yield a reorganization energy of ∼10 kcal mol^{-1}.

calculated to be considerably smaller then the reorganization energy of the heme in water (8.2 and 9.8 kcal mol^{-1} for the neutral and ionized model, respectively). If we exclude the contribution of the two ligands of the heme (His18 and Met80) that is designated by $\langle \Delta V_{QQ} \rangle$, λ_p becomes even smaller (4.6 and 6.3 kcal mol^{-1} for the neutral and ionized model, respectively). This finding supports our view that the protein is designed to reduce the reorganization energy. Treating the protein with its ionizable groups in their ionized state does not change the results drastically, in agreement with our earlier conclusions (Appendix C in ref 4).

In order to better understand the nature of the protein reorganization energy, it is useful to estimate the contributions of different groups to this quantity. The evaluation of group contributions is not unique and depends on the definition used (see ref 43 for discussion). Nevertheless, it is possible to define a group contribution as the effect of "mutating" the residual charges of the residue to zero. Muegge et al.[43] have shown that a reasonable estimate of the contribution of neutral residues can be obtained by taking the corresponding contribution to $\langle \Delta V_{q\mu}^{p} \rangle$ and dividing it by an effective "dielectric constant" (ϵ_p) with $\epsilon_p \approx 4$. It is important to note that ϵ_p does not represent the true local dielectric constant but a scaling factor that incorporates all the contributions that are not taken into account explicitly in this simplified approach. The approximation of $\epsilon_p = 4$ is not valid for charged residues, for which a scaling factor of $\epsilon_p = \epsilon_{eff} = 40$ has been chosen. This approximation has been validated repeatedly in previous studies (see refs 43 and 44 and references therein). Thus we used $[\langle \Delta V_{q\mu}^{p} \rangle_{i,ox} - \langle \Delta V_{q\mu}^{p} \rangle_{i,red}]/\epsilon_p$ with $\epsilon_p = 4$ for neutral groups and $\epsilon_p = 40$ for ionized groups as an estimate of the contribution of the *i*th group of the protein to the total reorganization energy. The result of this analysis is summarized in Figure 5. The contributions of the six internal NMR-detected water molecules are also shown in the figure. One can see that the contribution of these waters cannot be ignored. Note that the region around the highly conserved residue Ile81 contributes significantly to the reorganization energy. This will be discussed below together with the interpretation of the contributions of the protein residues to the redox potential.

In considering the nature of the protein reorganization energy, it is useful to examine how the overall structural change of the protein interacts with the heme. This issue can be analyzed in a qualitative way by evaluating the electrostatic potential *from the protein* at the locations of the heme atoms (see also ref 4). Such an analysis is presented in Figure 6, which depicts the electrostatic potential from the positively charged ($Q_{tot} = 2$) protein environment at the van der Waals surface of the heme. This potential was calculated using the PDLD approach as implemented in POLARIS.[38] Positive potential is colored in blue whereas zero potential is colored in red. As seen from the figure, the overall trend is such that the positive charge that develops upon oxidation is more stabilized by the oxidized protein than by the reduced one. This, of course, is consistent with the physical requirement that the environment of such a charge will be polarized toward this charge. In proteins this is accomplished by reorientation of the permanent dipoles of the protein residues and the solvent molecules in and around the protein. The reader might wonder why we do not have any point with a negative potential in Figure 6. This is due to the fact's that two negatively charged propionic acids are modeled as part of the heme and the protein net charge is +2e (the overall protein−heme system is neutral).

B. FEP Analysis of the Reorganization Energy. The current LRA approach and the geometrical mapping method used by Churg et al. and Warshel et al.[4,45] offer convenient ways of imposing structural constraints on calculations of reorganization energies.[46] The situation is somewhat more complicated if one uses the FEP/umbrella sampling approach of eq 4 to evaluate the Marcus parabolas. In this case it is not entirely clear how to force the system to satisfy the structural constraints imposed by the observed structure. The problem is to force the system to be near $\mathbf{r}_{ox}^{0}$ at the initial state and near $\mathbf{r}_{red}^{0}$ at the

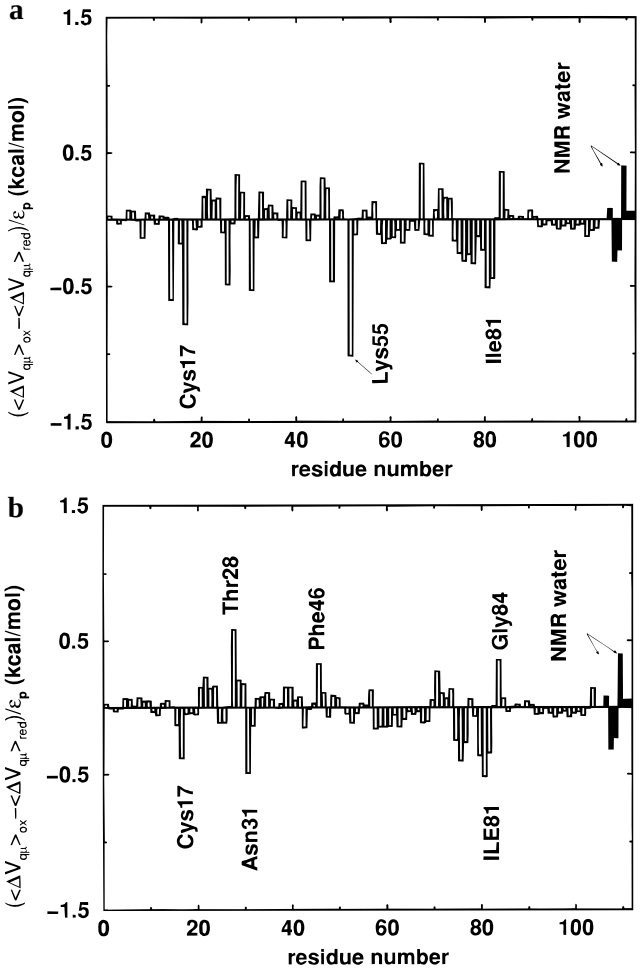

Figure 5. The contributions of the individual protein residues to the total reorganization energy for self-exchange between two cytochrome *c* molecules using the ionized protein model. Figure 5a shows the total contribution to the reorganization energy from each individual residue. The contribution is considered to be positive when the given residue stabilizes the oxidized heme. The filled bar charts (designated residue numbers 106−111) represent the contributions of the six internal water molecules defined by NMR (see refs 27 and 28). Figure 5b shows the contributions of the main-chain atoms, only.

final state even if the minima of the corresponding force fields do not coincide exactly with these solution structures. One way that may help to accomplish this is to add to the FEP mapping potential a term of the form $V'_m = V'_{ox}(1 - \theta_m) + V'_{red}\theta_m$ (eq 9). Here, however, we prefer to use a less rigorous approach that forces the system to stay closer to the experimentally observed structures. That is, we performed our FEP/umbrella sampling approach while using $V'_{ox}(\mathbf{r}^0 = \mathbf{r}^0_{ox})$ for the first 5 mapping step and using $V'_{red}(\mathbf{r}^0 = \mathbf{r}^0_{red})$ for the last five steps. The calculations involved a relatively small constraint potential ($K = 0.1$ kcal mol^{-1} Å^{-2}). One effect of this treatment is that the sampled configurational space for the first five ensembles does not coincide with that for the last five ensembles. The trajectories that started from two different conformations ($\mathbf{r}^0_{ox}$ and $\mathbf{r}^0_{red}$) were constrained by both the boundary and the constraint potential mentioned above. Moreover, even without any constraint one should not expect to reach the same conformation of the protein starting from either structure within the time spent to generate the trajectories. Although the FEP approach in principle, is superior to the LRA in regular free energy simulations the latter provides a more trustworthy way of introducing the NMR-based solution structures in reorganization energy calculations since it relies on extended trajectories around $\mathbf{r}^0_{red}$ and $\mathbf{r}^0_{ox}$ rather than trying to move from one structure to another.

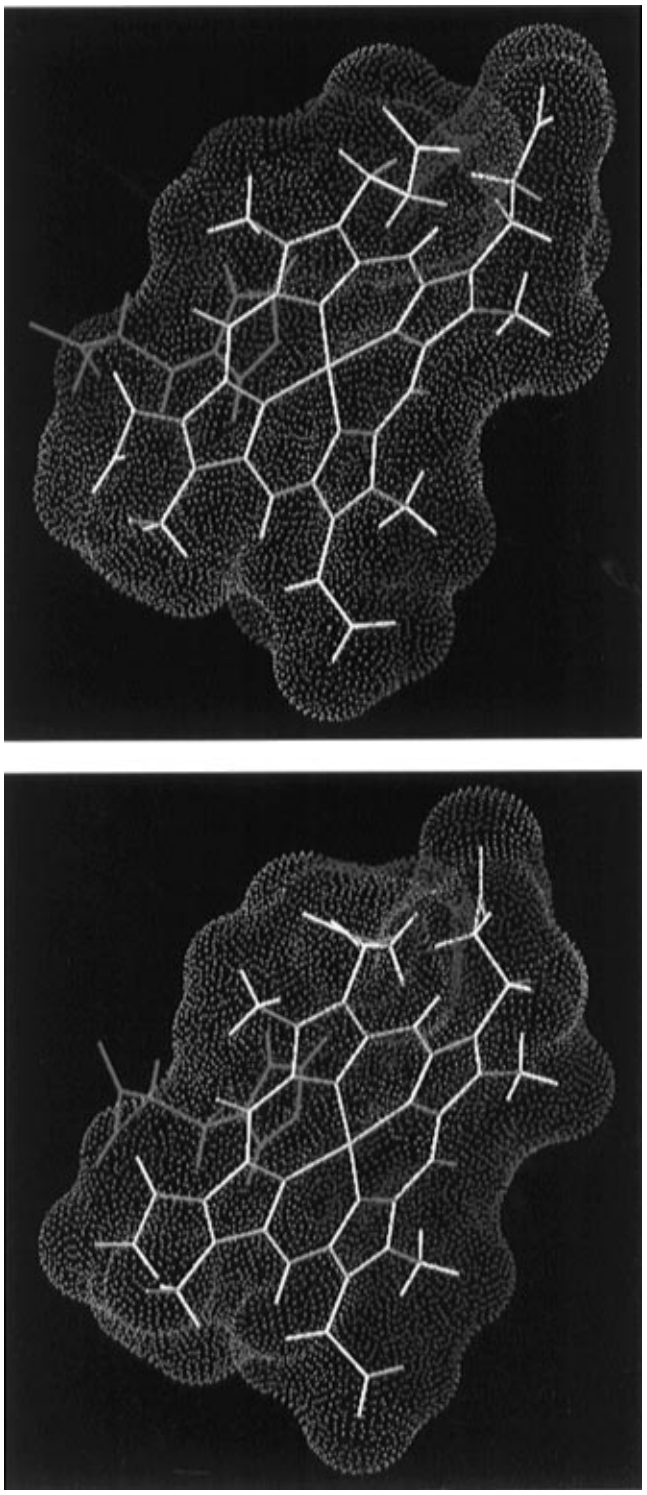

Figure 6. The electrostatic potential generated by the heme binding pocket on the van der Waals surface of the heme in ferro- (a) and ferricytochrome *c* (b). For the sake of clarity one heme ligand (His18) is shown in red. The potential surface was calculated using the protein dipole Langevin dipole (PDLD) approach as implemented in the program POLARIS.[38] The potentials obtained vary between 100 kcal mol^{-1} (blue) and zero (red). There is no negative potential represented in the color range since the protein matrix is positively charged in the ionized model (the heme bears negative charges from the propionic acids but we calculate the potential from the protein at the heme site rather then the potential from the heme itself) and the entire potential range is therefore shifted toward positive potential. See text for further discussion. The graphical interface of POLARIS 3.2 provided by Molecular Simulations has been used.

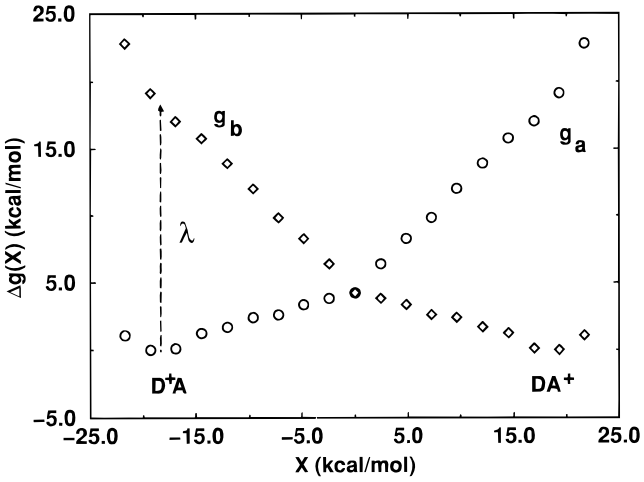

Figure 7. Free energy functions $\Delta g_a(X)$ and $\Delta g_b(X)$ for electron transfer between two cytochromes at infinite separation, obtained using the FEP/umbrella sampling method (eq 4). λ represents the reorganization energy of the ET reaction. The neutral protein model with $K = 0.1$ kcal mol^{-1} Å^{-2} was used. 11 surfaces were constructed with $0 \le \theta_m \le 1.0$ (eq 3). The total time spent for the generation of the trajectories after 20 ps of equilibration was 100 ps. The nonparabolic shape and the bend of the curves are an artifact of the specific constraints imposed on the cytochrome structures as explained in the text.

Figure 7 shows the calculated free energy functions for the ET process between two cytochromes at infinite separation using the neutral protein model. The reorganization energy λ^{∞}_{1-5} is estimated by this method to be 19.1 kcal mol^{-1}, in reasonable agreement with the estimate of 21.6 kcal mol^{-1} obtained by the LRA approach (Table 2). The nonparabolic shape of the curves and especially the bend at $X = 0$ is due to the imposed constraints. These constraints force the protein to stay relatively close to its oxidized (reduced) structure as the trajectories with $0 \le \theta_m \le 0.5$ ($0.5 < \theta_m \le 1.0$) are generated (see eqs 3 and 4). Although the curvatures of the free energy surfaces are not parabolic, the activation energy obtained from eq 1 and that obtained from the LRA approach ($\Delta g^{\ddagger} = \lambda/4 \cong 5$) coincide with the activation energy obtained from the FEP curves.

C. Macroscopic Estimates of Reorganization Energies. Although the main point of this work is the evaluation of λ by microscopic estimates, it is interesting to relate our findings to macroscopic models of electrostatic energies in proteins. This should allow us to examine the validity of such models and to determine the value and meaning of the corresponding dielectric constant. Here we exploit the advantage of having the "correct" energy contribution from microscopic LRA simulations. Thus, we can determine what dielectric constant should be used in the macroscopic model in order to reproduce the microscopic results. Our starting point is the macroscopic model of eq 19. This model can be quite arbitrary unless one has a unique way of determining the different phenomenological parameters. This can be accomplished by using the microscopic estimates of the solvation energies of the heme and the protein and the macroscopic Born formula. One can determine uniquely the effective values of $\bar{a}$ and $\bar{b}$ (eq 12) and can obtain from eq 19 (with $R \rightarrow \infty$)

$$\lambda^{\infty}_{\mathrm{mac}} \cong 166\frac{1}{\bar{a}}\left(1-\frac{2}{\bar{\epsilon}}\right)+166\frac{1}{\bar{b}}\left(\frac{2}{\bar{\epsilon}}-\frac{2}{80}\right)\cong\left[-\Delta G^{\mathrm{w}}_{\mathrm{sol}}(\mathrm{heme}^{\mathrm{red}}\rightarrow \mathrm{heme}^{\mathrm{ox}})\left(1-\frac{2}{\bar{\epsilon}}\right)-\Delta G^{3-4}_{\mathrm{sol}}\left(\frac{2}{\bar{\epsilon}}-\frac{2}{80}\right)\right]\left[\frac{1}{1-1/80}\right] \quad (21)$$

where $\Delta G^{\mathrm{w}}_{\mathrm{sol}}$ is the solvation energy of the oxidized heme−ligands system in water relative to that of the reduced system, and $\Delta G^{3-4}_{\mathrm{sol}}$ is the solvation energy of the oxidized protein relative to the solvation of its reduced form. The term [1/(1 − 1/80)] of eq 21 will be set equal to 1 in the analysis presented below and the term $^2/_{80}$ will be neglected.

TABLE 3: Calculated Redox Free Energy Obtained Using the LRA Approach

	model 1 $K = 0.1$, n, LPw[a]	model 2 $K = 50.0$, n, LPw	model 3 $K = 50.0$, i, LPw
$\Delta G^{\mathrm{w}}_{\mathrm{sol}}$ (no ind)	−30.7	−30.7	30.7
$\Delta G^{\mathrm{w}}_{\mathrm{sol}}$	−31.4	−31.4	−31.4
$\Delta G^{\mathrm{p}}_{\mathrm{sol}}$ (no ind)	−11.2	−6.5	−17.3
$\Delta G^{\mathrm{p}}_{\mathrm{sol}}$	−20.5	−21.7	−22.5
$\Delta\Delta G^{\mathrm{w}\rightarrow\mathrm{p}}$ (no ind)	19.5	24.2	13.4
$\Delta\Delta G^{\mathrm{w}\rightarrow\mathrm{p}}$ ($\Delta E^{\mathrm{p}}_{\mathrm{calc}}$)	10.9	9.7	8.9 (380)
$\Delta\Delta G^{\mathrm{w}\rightarrow\mathrm{p}}_{\mathrm{exp}}$ ($\Delta E^{\mathrm{p}}_{\mathrm{exp}}$)			7.3 (315)

[a] The protein atoms are harmonically constrained to their positions with the indicated force constant K (given in kcal mol^{-1} Å^{-2}). Free energies are given in kcal mol^{-1} and redox potentials in mV. $\Delta G^{\mathrm{w}}_{\mathrm{sol}}$, $\Delta G^{\mathrm{p}}_{\mathrm{sol}}$, and $\Delta\Delta G^{\mathrm{w}\rightarrow\mathrm{p}}$ are the free energy differences between the reduced and oxidized state of the heme of Lw, the free energy difference of LPw, and the difference between LPw and Lw, respectively. The calculated results are given with and without (no ind) contributions of induced dipoles. $\langle\Delta V_{\mathrm{intra}}\rangle$ and $\langle\Delta V_{QQ}\rangle$ have been omitted in the calculations since they have similar values in the protein and solution. However, in the ionized model (model 3), $\langle\Delta V^{\mathrm{prop}}_{\mathrm{intra}}\rangle$ has been included (compare to Table 1). $\Delta E^{\mathrm{p}}_{\mathrm{exp}}$ is the difference in redox potential between cytochrome *c* measured with respect to the standard hydrogen electrode (240 mV) and the corresponding value for the heme with its ligands (held by an octapeptide chain) in aqueous solution (−75 mV; see ref 45 and references therein). $\Delta\Delta G^{\mathrm{w}\rightarrow\mathrm{p}}_{\mathrm{exp}}$ is the free energy difference corresponding to $\Delta E^{\mathrm{p}}_{\mathrm{exp}}$.

Using $\Delta G^{\mathrm{w}}_{\mathrm{sol}}(\mathrm{heme}^{\mathrm{red}}\rightarrow\mathrm{heme}^{\mathrm{ox}}) \cong -31$ kcal mol^{-1} (Table 3) and $\Delta G^{3-4}_{\mathrm{sol}} \cong -6$ kcal mol^{-1} (where $\Delta G^{3-4}_{\mathrm{sol}}$ is the sum of the relevant $\Delta V^{\mathrm{w}}_{q\mu}$,$\Delta V^{\mathrm{w}}_{q\alpha}$,$\Delta V_{\mathrm{LD}}$ of Table 1), we obtain for the neutral protein case

$$\lambda^{\infty}_{\mathrm{max}} \cong 31\left(1-\frac{2}{\bar{\epsilon}}\right)+6\left(\frac{2}{\bar{\epsilon}}\right)\cong 31-\frac{50}{\bar{\epsilon}}=\lambda^{\infty}_{\mathrm{min}}=21 \text{ kcal mol}^{-1} \quad (22)$$

With the microscopic estimate of $\lambda^{\infty}_{\mathrm{mic}} \cong 21$ kcal mol^{-1} and by requiring that $\lambda^{\infty}_{\mathrm{mac}} = \lambda^{\infty}_{\mathrm{mic}}$, we obtain an estimate of $\bar{\epsilon} \approx$=5.0. The same treatment for the ionized protein gives $\bar{\epsilon} \approx 2.9$ (compare Tables 1, 2, and 3 for the corresponding values of $\Delta G^{\mathrm{w}}_{\mathrm{sol}}$, $\Delta G^{\mathrm{bulk}}_{\mathrm{sol}}$ and $\lambda^{\infty}_{\mathrm{mic}}$ that are given in kcal mol^{-1}).

The above estimate gives the "correct" protein dielectric constant expected from a consistent model that includes the protein dipolar groups as a part of the protein dielectric. This dielectric constant is the one used by Marcus and Sutin[37] and by Zhou.[47] However, the estimate of $\bar{\epsilon} \cong 10$ of Marcus and Sutin[37] is clearly an overestimate of the "dielectric constant" found here ($\bar{\epsilon} = 2.9$). The same conclusions emerge from the redox studies of the next section. It is also very important to realize that this dielectric constant is not equal (or even related directly) to the dielectric constant used in recent discretized continuum models,[48,49] which considers the protein dipoles explicitly (see discussion by King et al.[50] and also below). This dielectric constant (which will be discussed below) is referred to here as ϵ_{in}.

The low value for the dielectric constant of cytochrome *c* is consistent with the previous macroscopic estimates[45] and recent microscopic estimates[51,52] and is quite different from the dielectric constant of enzyme active sites.[50] This low dielectric

TABLE 4: Calculated Redox Energies Obtained Using the LRA/S Approach

	model 1 ($K = 0.1$, n, LPw[a])			model 2 ($K = 50.0$, n, LPw)			model 3 ($K = 50.0$, i, LPw)		
	$\langle\Delta V\rangle_{red}$	$\langle\Delta V\rangle_{ox}$	ΔG	$\langle\Delta V\rangle_{red}$	$\langle\Delta V\rangle_{ox}$	ΔG	$\langle\Delta V\rangle_{red}$	$\langle\Delta V\rangle_{ox}$	ΔG
$-\langle\Delta V^{w,\infty}\rangle$	4.1	57.3	30.7	4.1	57.3	30.7	4.1	57.3	30.7
$\langle\Delta V^{p}_{q\mu}\rangle + \langle\Delta V^{prop}_{intra}\rangle$	2.8	−8.8	−3.0	12.4	1.2	6.8	−12.3	−39.6	−26.0
$\langle\Delta V^{w}_{q\mu}\rangle$	0.4	−8.4	−4.0	−8.0	−9.0	−8.5	4.1	−1.4	1.4
$\langle\Delta V_{LD}\rangle$	5.3	−0.1	2.6	5.0	−0.9	2.1	0.9	0.1	0.5
$\langle\Delta G^{bulk}_{sol}\rangle$	−7.0	−6.8	−6.9	−6.9	−6.8	−6.8	6.8	6.8	6.8
$\Delta\Delta G^{w\to p}$			$19.4/\epsilon_{in}$			$24.2/\epsilon_{in}$			$13.4/\epsilon_{in}$
$\Delta\Delta G^{w\to p}$			9.7			12.1			6.7
(ΔE^{p})			(420)			(520)			(290)
$(\epsilon_{in} = 2)$									
$\Delta\Delta G^{w\to p}$			6.5			8.1			4.5
(ΔE^{p})			(280)			(350)			(190)
$(\epsilon_{in} = 3)$									

[a] The LRA/S approach scales the microscopic LRA results in the same way the PDLD/S scales the PDLD results (see text for discussion). The protein atoms are harmonically constrained to their positions with the indicated force constant K (given in kcal mol^{-1} Å^{-2}). The free energies and redox potentials are given in kcal mol^{-1} and mV, respectively. $(\Delta V^{w,\infty}\rangle$ represents the difference between the potential energy of the oxidized heme−ligand complexes in water. The meaning of the other terms is explained in Table 1. $\Delta\Delta G$ and ΔE are defined in Table 3. The lower part of the table gives the calculated redox free energy as a function of the assumed ϵ_{in}.

constant is also consistent with the requirement of low reorganization energy and with the requirement of destabilized oxidized heme as a way of controlling the redox potential (see below).

D. Estimating the Redox Potential from NMR Structures. The availability of NMR structures of the reduced and oxidized cytochromes provides a unique way for examining the relationship between the structural changes and the overall redox potential. Perhaps the most direct way of doing this is provided by the LRA approach used in the previous sections for the evaluation of λ. That is, as pointed out elsewhere,[45,53,54] one can express the redox potential in the protein in terms of the corresponding redox potential of the heme in water as

$$E_p = E_w - \Delta\Delta G^{w\to p}_{sol}/nF \tag{23}$$

where F is the Faraday constant. The change in solvation energy of the heme upon moving from water to the protein site can be written as (see eqs 6 and 8)

$$\Delta\Delta G^{w\to p}_{sol} = {}^1/_2[(\langle\Delta V^{p}\rangle_{ox} + \langle\Delta V^{p}\rangle_{red}) - (\langle\Delta V^{w}\rangle_{ox} + \langle\Delta V^{w}\rangle_{red})] \tag{24}$$

Using this expression, we obtain $\Delta\Delta G^{w\to p}$ of 8.9 kcal and a redox potential $\Delta E^{p}_{calc} = 380$ mV (see Table 3). This can be compared to experimental estimates of $\Delta\Delta G^{w\to p}_{exp} = 7.3$ kcal mol^{-1} and $\Delta E^{p}_{exp} = 315$ mV that represent the difference between the reduction potential of cytochrome *c* measured with respect to the standard hydrogen electrode (240 mV) and the corresponding value of the heme with its ligands in aqueous solution (−75 mV).

Another way to evaluate the protein redox potential involves upgrading the semimicroscopic PDLD/S approach[38] to the corresponding LRA/S approach. In this approach the protein permanent dipoles are treated explicitly, but the effect of the protein induced dipoles and the reorientation of the protein permanent dipoles are accounted for by a dielectric constant ϵ_{in}. Note that this dielectric is different than $\bar{\epsilon}$ of the previous section. The electrostatic energy $\Delta\Delta G^{w\to p}_{sol}$ is evaluated by the same cycle used in the PDLD/S derivation,[34] but the PDLD terms are replaced by the corresponding LRA terms. In the specific case of charge formation we obtain

$$\Delta\Delta G^{w\to p}_{sol} = -\Delta G^{w}_{sol}\left(\frac{1}{\epsilon_{in}} - \frac{1}{80}\right) + \Delta G^{p}_{q\mu}\left(\frac{1}{\epsilon_{in}}\right) + \Delta G^{3-5}_{sol}\left(\frac{1}{\epsilon_{in}} - \frac{1}{80}\right) \tag{25}$$

where the term ΔG^{3-5}_{sol} represents the solvation of the protein and heme system by the surrounding solvent, $\Delta G^{p}_{q\mu}$ is the interaction between the protein residual charges (and ionized groups) and the solute charges, and $\Delta\Delta G^{w}_{sol}$ is the solvation energy of the heme and its ligands in water. The different ΔG terms (e.g., $\Delta G^{p}_{q\mu}$) are obtained by

$$\Delta G_i = {}^1/_2[(\Delta V_i)_{red} + (\Delta V_i)_{ox}] = \langle\Delta V_i\rangle \tag{26}$$

The redox energies obtained from eqs 23 and 25 are summarized in Table 4. Again we obtain reasonable agreement between the calculated and observed redox potentials.

E. Determining the Dielectric Constant of Different Models. It is important to recognize that eq 25 takes into account, consistently, the protein reorganization energy while this does not seem to be the case in current macroscopic studies[47,48] that simply consider an observed protein structure or a protein configuration obtained after some relaxation of a single charge state (rather than two charge states) of the protein. If the protein reorganization is neglected, then ϵ_{in} is related to the ϵ used in most recent discretized continuum studies (e.g., those of Sharp and Honig[48]) while the above mentioned $\bar{\epsilon}$ is the one used by Zhou[47] and Marcus and Sutin.[37] Apparently, as we have argued previously, ϵ_{in} is not a universal parameter and has very little to do with the Kirkwood−Tanford protein dielectric constant $\bar{\epsilon}$ obtained when the permanent dipoles are treated as a part of the dielectric[44,50] (this is the dielectric used in eq 21 and the analysis of Marcus and Sutin[37]). In order to illustrate this nontrivial point, we compare below the $\bar{\epsilon}$ and ϵ_{in} that should be used in the corresponding redox models.

If one describes the totality of the protein by $\bar{\epsilon}$ one would obtain[46]

$$\Delta\Delta G^{w\to p}_{sol} = 166\left[-\frac{1}{\bar{a}}\left(1 - \frac{1}{\bar{\epsilon}}\right) - \frac{1}{\bar{b}}\left(\frac{1}{\bar{\epsilon}} - \frac{1}{80}\right) + \frac{1}{\bar{a}}\left(1 - \frac{1}{80}\right)\right] = \frac{-\Delta G^{w}_{sol}}{\bar{\epsilon}} + \frac{\Delta G^{3-5}_{sol}}{\bar{\epsilon}} \tag{27}$$

Similarly, if the protein is described by ϵ_{in} then the corresponding $\Delta\Delta G_{sol}^{w\rightarrow p}$ is given by eq 25. By comparing eqs 25 and 27 and neglecting terms of (1/80) of Equation 25, we obtain

$$\frac{-\Delta G_{sol}^{w}}{\epsilon_{in}} + \frac{1}{2}\left[\frac{(\Delta V_{sol}^{3-5} + \Delta V_{q\mu}^{p})_{ox} + (\Delta V_{sol}^{3-5} + \Delta V_{q\mu}^{p})_{red}}{\epsilon_{in}}\right] \quad (28)$$

$$= \frac{-\Delta G_{sol}^{w}}{\bar{\epsilon}} + \frac{\Delta G_{sol}^{3-5}}{\bar{\epsilon}} = \Delta\Delta G_{sol}^{w\rightarrow p}$$

where we used the definitions $\Delta G_{sol}^{w} = {}^{1}/_{2}(\langle\Delta V_{sol}^{w}\rangle_{ox} + \langle\Delta V_{sol}^{w}\rangle_{red})$. ϵ_{in} and $\bar{\epsilon}$ are identical when the protein contribution of the permanent dipoles ($\Delta V_{q\mu}^{p}$) is neglected, but when this contribution is included one obviously obtains different ϵ's and when $\Delta\Delta G_{sol}^{w\rightarrow p}$ is negative, as is the case, for example, in many iron−sulfur proteins,[55] there is no positive $\bar{\epsilon}$ that can produce the relevant results. In the present case we obtain $\Delta G_{sol}^{w} = -31.4$ kcal mol^{-1}, $\langle(\Delta V_{sol}^{3-5} + \Delta V_{q\mu}^{p})\rangle = -6.1$ kcal mol^{-1} where $\langle\ \rangle$ designates the average over the reduced and oxidized contributions. Thus, for the protein without ionized residues where $\Delta\Delta G_{sol}^{w\rightarrow p} \cong 9.7$ kcal mol^{-1} and $\Delta G_{sol}^{3-5} = -12.9$ kcal mol^{-1}, we obtain, by equating the left hand side of eq 28 to $\Delta\Delta G_{sol}^{w\rightarrow p}$, $((31.4-6.1)/\epsilon_{in}) = 9.7$ or $\epsilon_{in} = 2.6$. At the same time, we obtain from the right hand side of eq 28 $((-12.9 + 31.4)/\bar{\epsilon}) = 9.7$ and $\bar{\epsilon} = 1.9$. For the ionized protein case (including the interaction of the charged propionic acids with the heme ($\langle\Delta V_{intra}^{prop}\rangle$), we obtain $\epsilon_{in} = 1.5$ and $\bar{\epsilon} = 4.4$. Obviously, as demonstrated here, $\bar{\epsilon}$ and ϵ_{in} are not identical or related to each other by any simple concept.

Some readers might assume that the above examination of the meaning of the dielectric constant is just an exercise in computer modeling. However, deducing dielectric constants in different regions of the protein from microscopic simulations is at present the only way of determining the value of these parameters. The fact that the microscopic model may not be completely reliable is not relevant here since we like to know what is the proper dielectric for the given model as no other definition has a clear meaning (one cannot "measure" ϵ_{in} by any experiment since it is simply a reflection of the model used).

F. Group Contributions to Reorganization Energy and Redox Potential. Using the LRA approach we can examine the group contributions to reorganization energy (see also subsection A of this section) and the redox potential (Figures 5 and 8). The contribution to the redox potential can be obtained from sum of $\langle\Delta V\rangle_{red}$ and $\langle\Delta V\rangle_{ox}$. Figure 8 depicts these contributions for the ionized protein model, giving the total group contributions in Figure 8a and the corresponding main chain contributions in Figure 8b. The group contributions were calculated using the approach discussed above. The heme ligands His18 and Met80 provide the largest group contributions to redox potential. The charged side chains of Lys55 and Lys79 seem to lower ΔG. The involvement of Lys79 is particularly noteworthy as this residue is involved in a redox-dependent structural rearrangement that includes the highly conserved residue Ile81.[28] In the reduced protein, there is a bisection of the solvent accessible surface area of the heme edge by the side chain of Ile81. This is absent in the oxidized protein where the side chain of Ile81 is restricted to one side of the heme. Examination of the contributions to the reorganization energy reveals a large negative contribution from Ile81. This means that the redox dependent structural change of this residue and its neighbors reduces the activation barrier and accelerates the ET process. Since Ile81 is connected to Lys79 that participates in both determining the redox and the reorganization process,

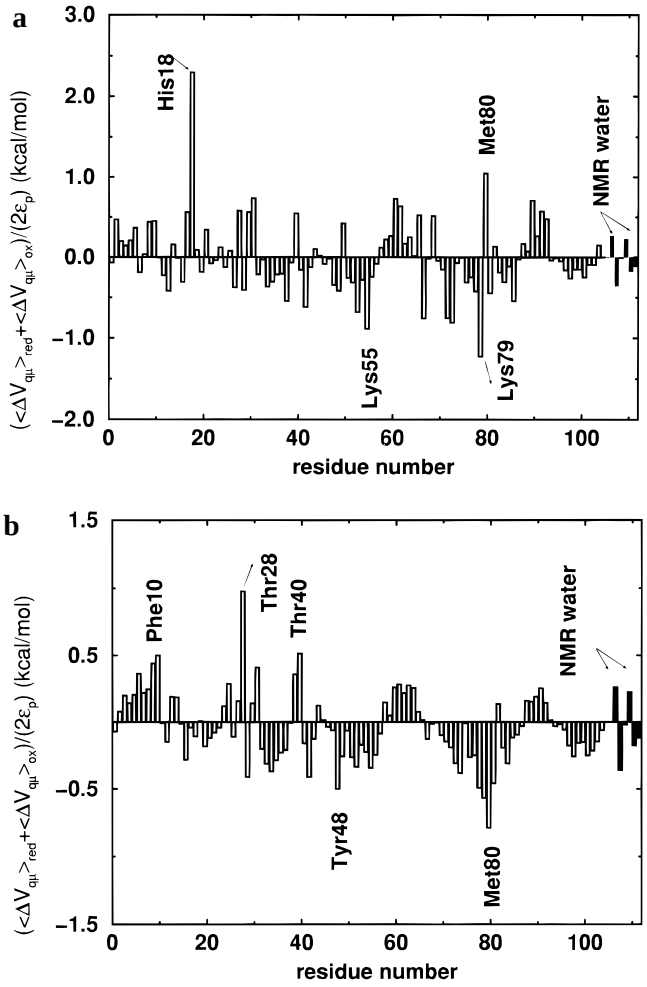

Figure 8. The contributions of (a) each individual amino acid residue of cytochrome *c* and (b) their main chain contributions to the arithmetic mean of $\langle\Delta V\rangle_i$ with i = red and ox. The filled bar charts (residue numbers 106−111) correspond to the six internal water molecules determined by NMR (see refs 27 and 28). The ionized protein model was used.

we establish here a direct thermodynamic linkage between a fundamental function (electron transfer) and another (molecular recognition). Though it has been known for some time that this region of the surface of cytochrome *c* is involved in formation of complexes with physiological redox partners (see ref 56 and references therein), this is the first direct evidence of a thermodynamic linkage between a definitive redox-dependent structure change and the redox potential of the heme. A mechanism linking a structural change to the redox potential is more easily imagined than one employing only a dynamic component such as that implied by the "push-button trigger" mechanism proposed by Brayer and co-workers.[57]

4. Concluding Remarks

The reorganization energy of redox proteins is a major factor in the control of biological electron transfer reactions. Direct experiments to uniquely determine reorganization energies and to estimate the protein contribution to these energies are far from trivial. Yet the availability of the structures of the reduced and oxidized forms of the protein offers the possibility of estimating the reorganization energy using the observed structural changes.

This work reexamined the value of the reorganization energy of cytochrome *c* using the reduced and oxidized solution structures of the protein. This was done primarily by using the

linear response approximation, which provides a rigorous way of imposing structural constraints on reorganization energy calculations.

The calculated reorganization energy ($\lambda^R \equiv \lambda^R_{1-5}$) is found to be between 9 and 15 kcal mol^{-1} and the contribution of the protein to this energy was found to be around 8−10 kcal mol^{-1}. The calculated value of λ^R is much smaller than that of the reorganization energy for electron transfer between two hemes in water (about 37 kcal mol^{-1}). This finding is consistent with previous proposals stating that one of the major functions of the protein is to reduce the reorganization energy and thus to accelerate the electron transfer process.[4,16,58] Yet, the present estimate is significantly larger than a previous estimate that was based on the crystal structures of reduced and oxidized tuna cytochrome *c*. Churg et al.[4] found $\lambda^R = 6$ kcal mol^{-1} summarizing $\lambda_p \cong 2$ kcal mol^{-1} (our λ_{1-2}), $\lambda_{intra} = 1$ kcal mol^{-1} (the heme contributions which was neglected in the present work), and $\lambda_w \cong 3$ kcal mol^{-1} (our λ_{3-5}). The small water contribution reflected the assumption that $R = 8$ Å which is clearly smaller than $R = 2\bar{b}$ used here (54 Å). The difference between the two results could reflect improvements in the reliability of the structural information. More recent studies of yeast cytochrome *c* seem to show larger structural changes.

The present work estimates λ by taking the observed structural changes from the NMR solution structure at their face value. We also obtain similar results when the structural constraints are reduced ($K = 0.1$ in Table 2). The calculated value of λ can be used to evaluate the activation barrier for electron transfer between two identical cytochromes which are held at a fixed distance. In this case, $\Delta G_0 = 0$ and eq 1 gives $\Delta g^{\ddagger} = \lambda/4 \cong 5$ kcal mol^{-1}. One might wonder what is the relationship between the results of the present analysis and previous attempts to estimate the reorganization energy from kinetic measurements. The value of $\Delta g^{\ddagger}$ for exchange between two cytochromes has been estimated by Nocera et al.[58] to be smaller than 7 kcal mol^{-1} using Marcus' cross relation. The corresponding upper limit of the reorganization energy ($\lambda \leq 28$ kcal mol^{-1}) is significantly larger than our estimate. Similarly, the reorganization energy for ET between cytochrome *c* and cytochrome *c* peroxidase was estimated to be around 37 kcal mol^{-1} by Cheung et al.[20] who evaluated the change in the rate of ET upon substituting the heme of cytochrome *c* by porphyrin (heme without central iron and therefore no bonds to the axial ligands). However, it is hard to accept this estimate as a definitive determination of λ since the porphyrin is free to move in the protein pocket and is expected to have significantly larger reorganization energy than the heme. Furthermore, studies of ET between cytochrome *c* and cytochrome b5 gave a much smaller λ ($\lambda \cong 18$ kcal mol^{-1}).[21,59] It seems to us that kinetic-based estimates of a large λ for cytochrome *c* reflect, in addition to the actual reorganization energy, the energetics of bringing the donor and acceptor together to the effective distance for the electron transfer process. This is further complicated by the possibility of having several binding sites for interaction between donor and acceptor.

Considering the difficulties of a unique estimate of the reorganization energy of cytochrome *c* from kinetic measurements, we believe that the combined use of NMR results and the LRA analysis provide at present the most reliable information about this quantity. This is particularly true with respect to the contributions from the protein, which are found here to be quite small (about 5 kcal mol^{-1}), supporting the view that the protein's role is to reduce the reorganization energy. It is also important to point out in this respect that the separated contribution of the protein cannot be estimated by any direct experiment.

It is useful to consider a recent attempt to estimate λ using a continuum model. While the study of Zhou[47] considered the protein structure in its redox calculation, it did not consider any specific information about the protein in the calculation of λ and it used eq 16 rather than eq 19. This expression corresponds to an infinitely large protein so that only the heme effective radius and the assumed dielectric constant (in this case $\bar{\epsilon}$) enter into the calculations of λ_p. The difficulties with this approach are, first, that the model does not reflect the size of the protein, and, second, that as shown in this work, there is no a priori way to determine $\bar{\epsilon}$. In addition, this treatment does not reflect the microscopic effect of the protein permanent dipoles. Using a continuum model without explicit permanent dipoles (e.g., no hydrogen bonds) is to return to the fundamental shortcomings of the Kirkwood−Tanford model where charges cannot be more stable in proteins than in solution (see discussion in ref 60). This is not a major problem in the case of cytochrome *c*, where the oxidized heme is less stable than in water; this effect can indeed be accomplished by having a low dielectric around the heme. However, such a model leads to an entirely incorrect physics in cases of redox proteins that stabilize their cofactors more than water does (e.g., the ferredoxins studied by Langen et al.[55]). Thus, such a model will be unable to reproduce the redox potential of ferredoxins and will require an entirely different ϵ for redox calculations and for estimating the reorganization energy. It is also instructive in this respect that the estimate of $\bar{\epsilon} \approx 10$ of Marcus and Sutin[37] is significantly larger than the current estimate ($\bar{\epsilon} = 2.9$). Thus, it seems to us that macroscopic calculations with an assumed ϵ cannot be used to determine reorganization energies. Of course, one can use microscopically calculated reorganization energies to estimate the effective ϵ (as is done here). Finally, it is useful to reiterate here that the ϵ that reproduces the protein reorganization energy does not have to correspond to the "correct" macroscopic $\bar{\epsilon}$ of the cytochrome (this latter ϵ can be deduced from microscopic simulations[31,51,52]).

The present work also used structural information to directly estimate the redox potential of the protein. The calculations reproduce the observed redox potential in a reasonable way by both the microscopic and semimicroscopic LRA methods. This is encouraging since both approaches can be used to evaluate redox potentials of other proteins. Furthermore, the present study afforded an opportunity to examine the meaning and magnitude of the dielectric constants obtained by different definitions. This analysis is independent of the difficulty of obtaining direct experimental information, since it is entirely based on the relationship between the microscopic and macroscopic values, which is unique for each model (eq 28). Our study demonstrates that the dielectric constants that correspond to different definitions can be quite different, as was argued in earlier discussions (e.g., refs 44 and 61). This conclusion implies that "pure" continuum treatments (that represent the protein by $\bar{\epsilon}$) cannot provide definitive information about redox energies. However, semimicroscopic treatments that represent a large part of the protein polarity in an explicit way can provide more unique information. This is particularly true when one takes into account explicitly the structural changes upon oxidation and uses the phenomenological dielectric only for an implicit representation of induced dipoles.

Finally it is useful to comment on the general issue of the optimization of λ in electron transport proteins. Let us start by addressing the question of whether or not the reorganization energies of biological couples are "unusually" small.[21] This question can only be examined by comparing the reorganization energies of the prosthetic groups in proteins to the reorganization

energy of the same prosthetic groups at the same distance but in water. It is hard to accomplish this comparison in a conclusive way by the available experimental approaches, but when the comparison is done using computer simulation approaches (as in the present work), one finds that λ is indeed significantly smaller in proteins than in water. Of course, when the distance between the donor and acceptor is very large, as in the case with cytochrome *c* and cytochrome *c* peroxidase (where the distance between the heme centers is about 23 Å), the protein cannot help too much, since the solvent contribution becomes dominant. However, when the distance is small (e.g., cytochrome *c* and cytochrome b5[21]) there is a significant advantage of having a small protein reorganization energy. Since cytochrome *c* is used in many biological functions, it is likely that the protein was optimized by evolution to have a small reorganization energy in cases where this small value is advantageous.

Acknowledgment. This work was supported by NIH Grants GM-40283 to A.W. and GM-35940 to A.J.W. I.M. greatly acknowledges support by a fellowship of the Deutsche Forschungsgemeinschaft.

References and Notes

(1) Marcus, R. A. *J. Chem. Phys.* **1956**, *24*, 966.
(2) Marcus, R. A. *J. Chem. Phys.* **1956**, *24*, 979.
(3) Marcus, R. A. *Annu. Rev. Phys. Chem.* **1964**, *15*, 155.
(4) Churg, A. K.; Weiss, R. M.; Warshel, A.; Takano, T. *J. Phys. Chem.* **1983**, *87*, 1683.
(5) Kuki, A.; Wolynes, P. G. *Science* **1987**, *236*, 1647.
(6) Warshel, A.; Parson, W. W. *Annu. Rev. Phys. Chem.* **1991**, *42*, 279.
(7) Beratan, D. N.; Onuchic, J. N.; Winkler, J. R.; Grey, H. B. *Science* **1992**, *256*, 1740.
(8) Gruschus, J. M.; Kuki, A. *J. Phys. Chem.* **1993**, *97*, 5581.
(9) Kowalski, A. *Biochemistry* **1965**, *4*, 2382.
(10) Redfield, A. G.; Gupta, R. J. *Cold Spring Harbor Symp. Quant. Biol.* **1971**, *36*, 405.
(11) Mayo, S. L.; Ellis, W. R., Jr.; Crutchley, R. J.; Grey, H. B. *Science* **1986**, *233*, 948.
(12) Churg, A. K.; Warshel, A. In *Structure & Motion: Membranes, Nucleic Acids & Prtoteins;* Clementi, M. H., Sarma, R. H., Eds.; Academic Press: New York, 1985; p 361.
(13) Friesner, R. *Structure* **1994**, *2*, 339.
(14) Takano, T.; Dickerson, R. E. *J. Mol. Biol.* **1981**, *153*, 79.
(15) Takano, T.; Dickerson, R. E. *J. Mol. Biol.* **1981**, *153*, 95.
(16) Warshel, A.; Schlosser, D. W. *Proc. Natl. Acad. Sci. U.S.A.* **1981**, *78*, 5564.
(17) Yadav, A.; Jackson, R. M.; Holbrook, J. J.; Warshel, A. *J. Am. Chem. Soc.* **1991**, *113*, 4800.
(18) Moser, C. C.; Keske, J. M.; Warncke, K.; Farid, R. S; Dutton, P. L. *Nature* **1992**, 355, 796.
(19) Farid, R. S.; Moser, C. C; Dutton, P. L. *Curr. Opin. Struct. Biol.* **1993**, *3*, 225.
(20) Cheung, E.; Taylor, K.; Kornblatt, J. A.; English, A. M.; McLendon, G.; Miller, J. R. *Proc. Natl. Acad. Sci. U.S.A.* **1986**, *83*, 1330.
(21) McLendon, G. *Acc. Chem. Res.* **1988,** *21*, 160.
(22) Wand, A. J.; Englander, S. W. *Biochemistry* **1985**, *24*, 5290.
(23) Wand, A. J.; DiStefano, D. L.; Feng, Y.; Roder, H.; Englander, S. W. *Biochemistry* **1989**, 28, 186.
(24) Feng, Y.; Roder, H.; Englander, S. W. *Biochemistry* **1990,** *27*, 3494.
(25) Feng, Y.; Roder, H.; Englander, S. W.; Wand, A. J.; DiStefano, D. L. *Biochemistry* **1989**, *28*, 195.
(26) Qi, P. X.; DiStefano, D. L.; Wand, A. J. *Biochemistry* **1994**, *33*, 6408.
(27) Qi, P. X.; Urbauer, J. L.; Fuentes, E. J.; Leopold, M. F.; Wand, A. J. *Nat. Struct. Biol.* **1994**, *1*, 378.
(28) Qi, P. X.; Beckman, R. A.; Wand, A. J. *Biochemistry* **1996**. In press.
(29) Warshel, A. *J. Phys. Chem.* **1982**, *86*, 2218.
(30) Hwang, J.-K.; Warshel, A. *J. Am. Chem. Soc.* **1987**, *109*, 715.
(31) King, G.; Warshel, A. *J. Chem. Phys.* **1990,** *93*, 8682.
(32) Kuharski, R. A.; Bader, J. S.; Chandler, D.; Sprik, M.; Klein, M. L.; Impey, R. W. *J. Chem. Phys.* **1988**, *89*, 3248.
(33) Papazyan, A.; Maroncelli, M. *J. Chem. Phys.* **1991**, *95*, 9219.
(34) Lee, F. S.; Chu, Z. T.; Bolger, M. B.; Warshel, A. *Protein Eng.* **1992**, *5*, 215.
(35) Åqvist, J.; Medina, C.; Samuelsson, J.-E. *Protein Eng.* **1994,** *7*, 385.
(36) Levy, R. M.; Belhadj, M.; Kitchen, D. B. *J. Chem. Phys.* **1991**, *95*, 3627.
(37) Marcus, R. A.; Sutin, N. *Biophys. Biochim. Acta* **1985,** *811*, 265.
(38) Lee, F. S.; Chu, Z. T.; Warshel, A. *J. Comp. Chem.* **1993**, *14*, 161.
(39) Warshel, A.; Lappicirella, A. *J. Am. Chem. Soc.* **1981**, *103*, 4664.
(40) Lee, F. S.; Warshel, A. *J. Chem. Phys.* **1992**, *97*, 3100.
(41) Luzhkov, V.; Warshel, A. *J. Comp. Chem.* **1992,** *13*,199.
(42) The use of eq 20 for the ionized protein model is not fully justifiable since such a continuum model is not expected to properly present this system. This reflects the fact that the contribution of the ionized groups in region 2 is compensated for by the solvent in regions 3−5. This effect is not captured by the oversimplified model of Figure 3 and eq 19. In fact, we feel that the actual distance dependence of λ in a given donor−acceptor pair should be determined by realistic calculations rather than by eq 20. Moreover, most biological donor−acceptor pairs involve complementary surface charges that neutralize each other. The corresponding distance dependence is not expected to be the same as the one evaluated here for two identical cytochromes.
(43) Muegge, I.; Schweins, T.; Langen, R.; Warshel, A. *Structure* **1996**, *4*, 475.
(44) Warshel, A.; Åqvist, J. *Annu. Rev. Biophys. Biophys. Chem.* **1991**, *20*, 267.
(45) Churg, A. K.; Warshel, A. *Biochemistry* **1986**, *25*, 1675.
(46) The original approach of Churg et al.[4] estimated the reorganization energy by defining a reaction coordinate along the vector that connected the crystal structures of the reduced and oxidized cytochromes. Of course, the use of this effective coordinate is not identical to rigorous free energy perturbation calculations.
(47) Zhou, H.-X. *J. Am. Chem. Soc.* **1994**, *116*, 10362.
(48) Sharp, K. A.; Honig, B. *Annu. Rev. Biophys. Biophys. Chem.* **1990**, *19*, 301.
(49) Bashford, D.; Karplus, M. *Biochemistry* **1990**, *29*,10219.
(50) King, G.; Lee, F. S.; Warshel, A. *J. Chem. Phys.* **1991**, *95*, 4366.
(51) Simonson, T.; Perahia, D. *Proc. Natl. Acad. Sci. U.S.A.* **1995**, *92*, 1082.
(52) Simonson, T.; Perahia, D. *J. Am. Chem. Soc.* **1995**, *117*, 7987.
(53) Parson, W. W.; Chu, Z. T.; Warshel, A *Biochim. Biophys. Acta* **1990**, *1017*, 251.
(54) Langen, R.; Brayer, G. D.; Berghuis, A. M.; McLendon, G.; Sherman, F.; Warshel, A. *J. Mol. Biol.* **1992**, *224*, 589.
(55) Langen, R.; Jensen, G. M.; Jacob, U.; Stephens, P. J.; Warshel, A. *J. Biol. Chem.* **1992**, *267*, 25625.
(56) Pelltier, H.; Kraut, J. *Science* **1992**, *258*, 1748.
(57) Berghuis, A. M.; Brayer, G. D. *J. Mol. Biol.* **1992**, *223*, 959.
(58) Nocera, D. G.; Winkler, J. R.; Yocom, K. M.; Bordignon, E.; Gray, H. B. *J. Am. Chem. Soc.* **1984**, *106*, 5145.
(59) It is useful to point out in this respect that the reorganization energy for ET from pheophytin to quinone in bacterial reaction centers is around 15 kcal mol^{-1}.[62] This relatively small λ is of some relevance since in this case it was possible to estimate λ by a systematic variation of the thermodynamic driving force and since the donor and acceptor are kept at constant distance.
(60) Warshel, A.; Russell, S. T.; Churg, A. K. *Proc. Natl. Acad. Sci. U.S.A.* **1984**, *81*, 4785.
(61) Warshel, A.; Russell, S. T. *Q. Rev. Biophys.* **1984**, *17*, 283.
(62) Gunner, M. R.; Robertson, D. E.; Dutton, P. L. *J. Phys. Chem.* **1986**, *90*, 3783.